Hindawi Publishing Corporation
Journal of Nanomaterials
Volume 2012, Article ID 691874, 6 pages
doi:10.1155/2012/691874

Research Article

Single-Crystal MgO Hollow Nanospheres Formed in RF Impulse Discharge Plasmas

Satoru Iizuka and Takumasa Muraoka

Department of Electrical Engineering, Graduate School of Engineering, Tohoku University, Aza-Aoba 6-6-05, Aramaki, Aoba, Sendai 980-8579, Japan

Correspondence should be addressed to Satoru Iizuka, iizuka@ecei.tohoku.ac.jp

Received 30 June 2011; Revised 25 October 2011; Accepted 28 October 2011

Academic Editor: Takuya Tsuzuki

Spherical MgO nanoparticles with a hollow inside, that is, MgO hollow nanospheres, were created in Ar/O_2 plasma produced by radio frequency (RF) impulse discharge using a Mg rod electrode. The hollow nanospheres were found on the SiO_2 plates placed near the powered Mg electrode. The electron refraction pattern showed that each nanosphere was made of a single crystal of MgO. Since the shape was spherical, these nanoparticles seemed to be created during the levitation in the plasma without touching any walls. The formation mechanism with a quasiliquid cooling model was also discussed.

1. Introduction

Magnesium oxide (MgO) has been utilized as a transparent film with favourable secondary electron emission coefficient for a flat plasma display panel [1]. MgO is also used as a buffer layer for the deposition of high T_c superconducting films and perovskite-type ferroelectric films. MgO has been widely used as a refractory material in steel manufacture because of its high corrosion resistance and high-melting point. MgO is also used as an optical transmitter and as a substrate for thin film growth. Various methods for the production of MgO films were reported [2–5], where various morphologies of MgO films, such as flat thin films, whiskers, fishbone fractal nanostructures, and nanofibers, were observed. Photoluminesence emission spectra in the UV range were dependent on the size of MgO nanoparticles [6].

Here, a special shape of MgO nanoparticles with a hollow space inside, that is, a hollow nanosphere or a spherical nanoshell, is reported. Moreover, each particle is made of a single crystal of MgO in spite of its spherical shape. This kind of structure can be used to form an optical scattering surface when they are coated on the surface homogeneously. The mass to volume ratio can be reduced compared to a conventional packed sphere. An improvement of electronic properties such as field electron emission efficiency might be expected. Another possible application includes packing of foreign materials in the hollow.

Concerning with the formation of hollow microspheres, several works have been reported. Ferrite hollow spheres were prepared and fabricated by coating ferrite nanoparticles on the surface of polystyrene spheres and removing of the core polymer subsequently [7]. SiO_2 hollow spheres were also prepared by heat treatment of a mixture composed of $SiCl_4$ and carbon microsphears [8]. Double shell hollow spheres were prepared by encapsulating the polymeric hollow spheres with a TiO_2 shell [9]. By using a pulsed laser deposition method, hollow ZnO spheres have been prepared after annealing the depositions [10]. All of these experiments employed an additional chemical and heat treatment. Recently, one-step synthesis of MgO hollow nanospheres were demonstrated by a pulsed-laser ablation method, where Mg target was melted, followed by surface oxidization [11]. However, only a simple sputtering method was employed in Ar/O_2 plasma without chemical and thermal processes. The formation technique was quite different from the above methods.

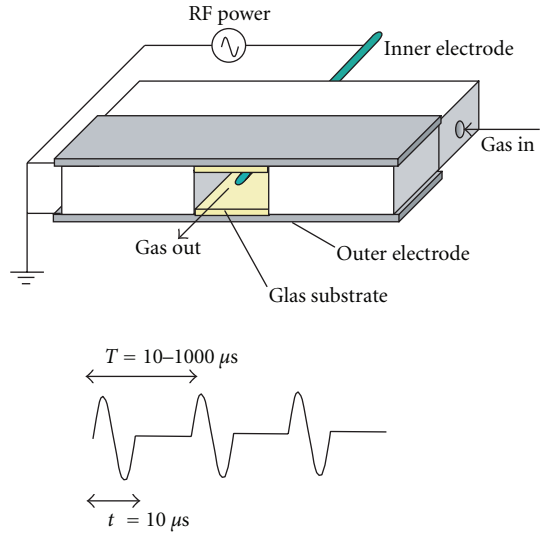

Figure 1: RF impulse discharge system with plate and rod electrodes. The gas was fed between glass plates with narrow gap where the electric impulse discharge takes place. Inset shows a waveform of the applied voltage.

2. Experimental Setup

The experimental configuration is shown in Figure 1 [12]. Using this system, deposition materials on the flat glass plates made of SiO_2 can be easily analysed. Two glass plates were placed with a narrow spacing gap as shown in Figure 1. The spacing between the glass plates was fixed at 2 mm. To ignite a discharge, a powered rod electrode was introduced between the two glass plates. Another two grounded stainless plate electrodes that sandwich the glass plates were also placed. The inner rod electrode was made of a Mg rod with a diameter of 1.7 mm. The outer stainless electrode was not fixed, so that the distance between the inner and outer electrodes could be varied in the axial direction. In this experiment, however, the distance between the inner and outer electrodes was fixed at 5 mm.

The entire electrode system shown in Figure 1 was set inside a cylindrical vacuum chamber of 50 cm in diameter and 20 cm in height. The working gases of Ar and O_2 were introduced into a mixing vessel through mass flow controllers independently, and finally the mixed gas was fed to the discharge region through a gas inlet tube connected to the inner electrode, as shown in Figure 1. The outgoing gas from the discharge region was directly drained into the chamber and evacuated by a rotary pump. Since the length of the glass plate was short ($\approx$10 mm), the pressure in the discharge region was nearly the same as that in the vacuum chamber. The pressure of the chamber was fixed at 0.1 Torr with a total gas flow rate of 20 sccm.

RF impulse voltage was directly supplied to the inner electrode through a coaxial cable without using a matching circuit and a blocking condenser, while the outer electrode is grounded. As shown in an inset of Figure 1, the RF impulse power supply provided one cycle of a sinusoidal waveform of 10 μs in width with the repetition frequency ω_R. The pulse amplitude and the repetition frequency can be changed. In this experiment, the pulse repetition frequency was fixed at 4.5 kHz. The applied voltage can be increased up to 20 kV.

The surface morphology was analysed by scanning electron microscopy (SEM) with a resolution of 5.0 nm and a maximum magnification of 300,000 (JCM-5700, JEOL). The transmission electron microscopy (TEM) analysis was also employed to analyse the crystal structure.

3. Experimental Results

Figure 2 shows SEM images of the depositions on the glass plate surface. Many small spherical particles were formed as shown in Figure 2(a). Typical size of the particles was 200–400 nm. Here, spherical nanoparticles with diameters less than 100 nm could be also observed. Figure 2(b) shows a SEM image in the direction perpendicular to the glass plate surface. The cross-sectional view of these particles indicates that these particles seem to be just put on the glass plate surface. So, it was supposed that these particles were formed during levitation in the plasma discharge, and fallen down and attached to the surface of the glass plate. It was also found that these nanospheres had a quite symmetrical ball structure, and so there was no indication that they were grown up on the surface of the substrate. Therefore, these particles should have grown in the plasma without touching any places. The dependence of the depositions on the experimental parameters was described in [13], together with [12].

In order to evaluate the structure of these spherical particles more in detail, a TEM image is shown in Figure 3, where several spherical nanoparticles can be observed. Note that most of particles are hollow spheres, although the size is not the same; that is, most of these nanoparticles are spherical and include spherical hollow inside. But, some of them have nonuniform shell thickness. In order to check the crystallite of those hollow spheres more in detail, a few particles were chosen as shown in Figure 4(a). The electron refraction pattern for these particles is shown in Figure 4(b), where narrow refraction spots can be clearly observed. In general, the relation $D = \lambda L/r(\mathrm{hkl})$ holds for the electron refraction, where D is radius of the refraction ring, L is the distance between the sample and screen, λ is de Brolie wavelength of the electron beam, and $r(\mathrm{hkl})$ is lattice position in the x, y, and z directions. It was obtained that $r(111) = 0.244$ nm, $r(200) = 0.211$ nm, $r(220) = 0.149$ nm, $r(311) = 0.127$ nm, $r(222) = 0.120$ nm, and $r(400) = 0.105$ nm. The positions of these spots are found to be exactly coincident with the radii of the rings related with the MgO with lattice constant $a = 0.4203$ nm. Therefore, it is concluded that each hollow spherical particle is made of a single crystal of MgO.

Figure 5 shows the relation between outer diameter D and inner hollow diameter d of MgO nanospheres. The hollow diameter d increases almost in proportion with an increase of the outer diameter D. From a straight line drawn in the figure, the ratio d/D was found to be about 0.6, and the ratio d/D was almost independent of the particle size;

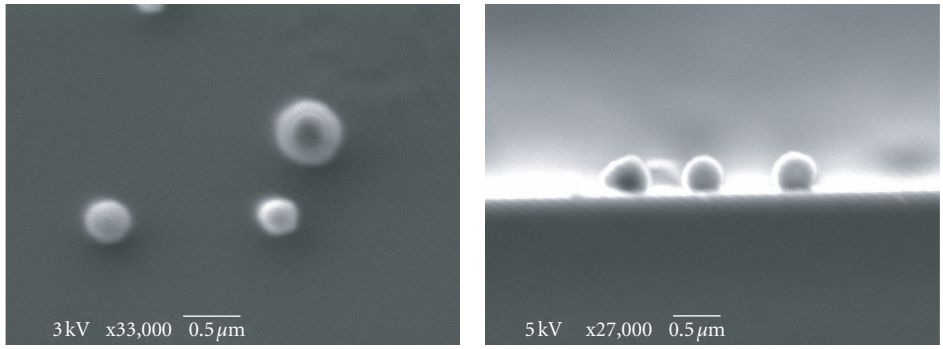

(a) (b)

Figure 2: SEM images of the nanoparticles deposited when Ar/O_2 mixing ratio is 3/1 and total pressure is 0.1 Torr. (a) top view, (b) side view. The particles are spherical shape.

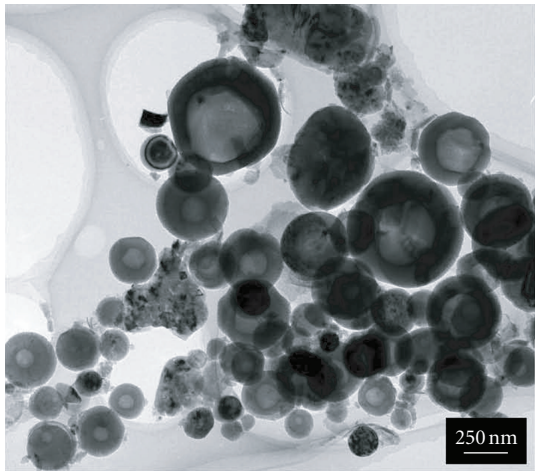

Figure 3: TEM images of nanoparticles deposited near the electrode when Ar/O_2 mixing ratio is 3/1 and total pressure is 0.1 Torr. The size of nanoparticles is distributed mostly in the range 50–500 nm. Most of particles have spherical hollow inside.

that is, larger particles had a larger hollow inside. However, most of the particles smaller than 50 nm seemed to have no detectable hollow inside. These phenomena would be closely related with the formation mechanism of the hollow nanospheres, as discussed in the next section.

The SEM image in the region of thick deposition is shown in Figure 6. It can be confirmed that the depositions are in principle consisted of many small nanoparticles. Moreover, a few particles in Figure 6 are found to have an open hole on the surface. This indicates that a thin part of the shell layer surrounding the particle has been broken by chance, and the inner hollow space was exposed through an open hole. This structure also confirms that these particles are basically hollow particles.

4. Discussion

Here, the formation mechanism of these hollow MgO nanospheres is discussed. A diffusion model of oxygen into a melted Mg nanosphere was proposed for a formation of MgO hollow nanosphere in pulsed-laser deposition [11]. During the cooling, oxygen in gas phase penetrated into Mg nanospheres to form a MgO layer on the surface. On the contrary, Mg atoms in the core region diffused toward the surface region, leaving a void in the core. This model could not be directly applied to the present study, because melted metallic Mg nanoparticles were not created initially. Instead, nanoparticles contain both Mg and O atoms from the beginning, because the reactions between Mg and O would occur immediately after Mg sputtering from the Mg rod electrode in the discharge plasma.

In this study, the following model was considered for a formation of hollow MgO nanospheres. Owing to the sheath potential in front of the Mg rod electrode during the discharge, Mg atoms are sputtered by energetic Ar ions. These Mg atoms react with O atoms in the plasma to form MgO nuclei. Such MgO nanoclusters would coagulate and grow in the plasma, and then nanoparticles containing Mg and O atoms were produced. Note that in the plasma, strong local electric filed occurs in front of the levitated nanoparticles due to a sheath formation. Therefore, Ar ions are accelerated towards the surface of nanoparticle and transfer kinetic energy to nanoparticles, then the nanoparticles will be heated up as discussed below and will reach a quasiliquid state. It was also noted that these nanoparticles were charged up negatively by an effect of electrons in the discharge. Therefore, they can be confined electrically within positive plasma potential for a long period. Since the nanoparticles are in quasiliquid state, the shape will be spherical, as schematically illustrated in Figure 7(a).

Since the impulse discharge was employed, these nanospheres would have a chance to escape from the discharge region during discharge off-interval. In this case, these particles will be in turn cooled down owing to the collisions with neutral Ar atoms before arriving at the surface of the glass plate. The solidification of nanoparticles will start from the particle surface, as shown in Figure 7(b). During this process, Mg atoms will be subtracted toward the surface for MgO crystal formation, because the number of Mg atoms would be lacked near the surface, compared

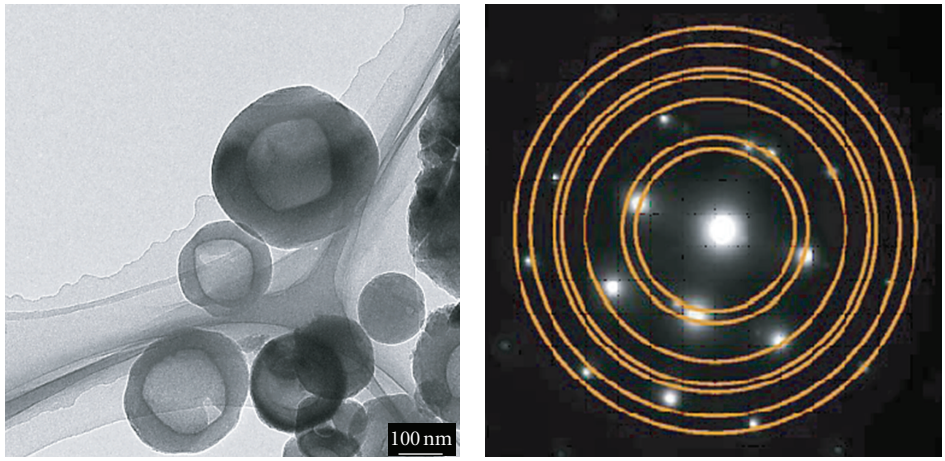

Figure 4: (a) TEM image of a few nanoparticles and (b) electron refraction pattern for these particles. The rings radii correspond to refraction positions for MgO crystal. This dotted pattern shows that the spherical hollow nanoparticles are consisted of single crystal of MgO.

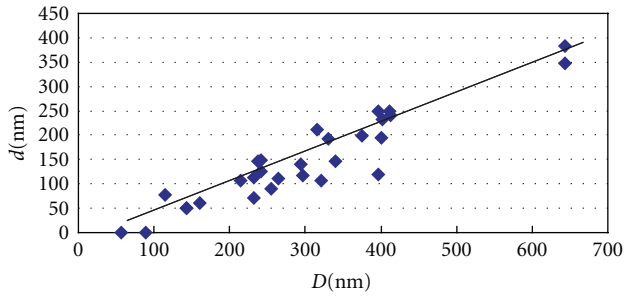

Figure 5: Relation between the diameters D and d of nanospheres and spherical hollow inside, respectively, for nanospheres deposited under the same condition in Figure 3. Solid line shows a slope of $d/D = 0.6$.

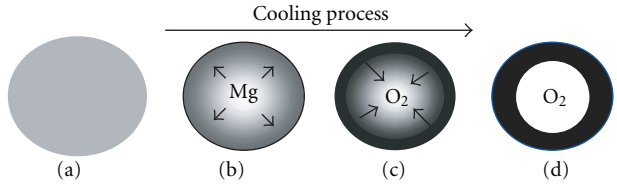

Figure 7: Cooling process of nanoparticles. Liquid, solid, and gas regions are drawn by grey, black, and white, respectively. (a) Liquid MgO droplets with spherical shape. (b) Outer surface starts being cooled down to form MgO crystal by collecting Mg atoms from the central core. (c) The crystallization proceeds toward the core by expelling excess oxygen toward the centre. (d) Hollow nanosphere of single crystal MgO.

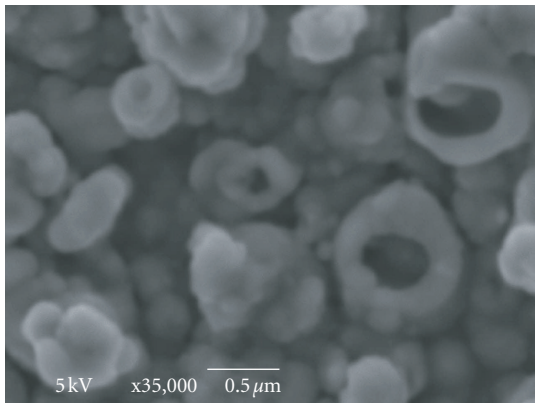

Figure 6: SEM images of nanoparticles deposited near the electrode when Ar/O_2 mixing ratio is 3/1 and total pressure is 0.1 Torr. There observed several nanoparticles with circular hole on the surface. These nanoparticles seem to be originally formed as hollow spheres.

with that of oxygen supplied from the gas phase. On the other hand, excess oxygen inside the nanoparticles will be expelled toward the melted core region, because outer surface was solidified and crystallized, as shown in Figure 7(c). This process will lead to a hollow inside filled with oxygen, as shown in Figure 7(d). Since the cooling process is rather slow, compared with the heating process, single crystal structure of MgO would be formed. Here, it is also noted that in the quasiliquid state, Mg and O will be ionised to form Mg^{2+} and O^{2-}, respectively. The electric force among these ions inside the nanoparticles may also play a key role for driving a collection of Mg^{+} toward the surface (see Figure 7(b)) and an expulsion of excess O^{-} toward the core (see Figure 7(c)) during crystal formation mentioned above.

The energy $W_i(J/s)$ transferred to the MgO nanoparticle of radius R per second can be estimated by ion bombardment

energy $E_i = eV_s$, and ion flux $J_i = n_i v_i$, that is, $W_i = S_p E_i J_i$, where S_p is the particle surface area ($=4\pi R^2$), n_i is ion density, $v_i = \sqrt{2eV_s/m_i}$ is ion velocity, and V_s is ion acceleration voltage in the sheath in front of the nanoparticle. On the other hand, the heat capacity H(J/°C) for increasing the particle temperature is expressed by $H = kM$, where k(J/kg°C) is specific heat, $M = (4/3)\rho_0 \pi R^3$ is mass, and ρ_0 is specific gravity of MgO. Of course, the other heating mechanisms, such as radiation heating and electron heating and also the other cooling mechanism such as the collisions with neutral Ar/O_2 gas should be also taken into account. Here, however, as a dominant mechanism, the effect of ion bombardment has to be discussed. In the case of a particle of $R = 3$ nm, for example, it is obtained that $\Delta T/\tau = 5.7 \times 10^2$ for the time τ required for increasing the particle temperature ΔT. This shows that an expose of particles to the plasma for $\tau = 3.6$ s will lead to an increase of particle temperature by about $\Delta T = 1000$°C. Here, the impulse discharge with repetition frequency $\omega_R = 4.5$ kHz, $V_s = 10\,V$, and $n_i = 5 \times 10^9/\text{cm}^3$ was taken into account. The temperature rises more quickly for smaller particles ($T/\tau \propto 1/R$). If the other heating mechanism mentioned above was considered, the temperature rise time might be much shorter. In a typical case, the discharge was continued for 10 minutes. Therefore, nanoparticles growing in the plasma would be heated up by the ion bombardment to reach a quasiliquid state.

The volume of such a quasiliquid spherical droplet of MgO shown in Figure 7(a) expands as a result of heating. During the cooling, solidification proceeds from the surface to the core region. Therefore, the outer diameter D of particles will be maintained, and only the particles in the core region will be rearranged to form a shell structure of MgO crystal, as shown in Figure 7(d). If the number of Mg atoms is preserved during the cooling, a relation $nV = n_0 V_0$ will be hold, where n is Mg density in the droplet, V ($=(4/3)\pi(D/2)^3$) is the droplet volume, n_0 is Mg density in MgO crystal, and V_0 ($=(4/3)\pi[(D/2)^3 - (d/2)^3]$) is the shell volume. Then, the relation $n/n_0 = V_0/V = 1-(d/D)^3 \approx 0.78$ can be obtained. Here, $d/D \approx 0.6$ is used from Figure 5. Therefore, the number ratio of atoms in the quasiliquid MgO droplet can be estimated to be Mg : O $\approx$ 1 : 1.28, containing excess oxygen. The density of Mg in the quasiliquid MgO droplet would be almost constant, independent of the particle size, as shown in Figure 5. This is consistent with the constancy of the ratio d/D.

A following trapping mechanism was considered for the nanoparticles levitated in the plasma. The forces acting on the charged nanoparticles levitated in plasmas were electrostatic force, ion drag force, thermophoresis, gravity, and neutral drag by the gas flow. Here, thermophoresis was negligible because of no heating. Since the nanoparticles were deposited on upper and lower sides of the glass plates placed parallel to the horizontal direction, the gravity was unimportant. Neutral drag by gas injection was also negligible because it acted mainly in the horizontal direction. Therefore, ion drag force would play a key role for the particle transport toward the glass plates.

5. Conclusion

In conclusion, RF impulse plasma was produced within a space between narrow glass plates using an Mg rod electrode system. It was found that hollow nanospheres were deposited on the glass plate surface. The particles were predominantly deposited on the glass substrate close to the inner Mg rod electrode. From the TEM image and electron refraction patterns, these hollow nanospheres were found to be composed with MgO single crystal. The average size of the particles was several 100 nm. Further, the formation processes of such spherical particles were discussed. A melting process of the particles by the ion bombardment was considered during the growth of MgO nuclei and cluster. Cooling process starting from the outer surface of the particles will confine excess oxygen in the core, resulting in formation of a hollow sphere made of MgO single crystal. It is demonstrated that the RF impulse discharge system employed here is very useful for the formation of MgO hollow nanospheres.

Acknowledgment

This work was partially supported by a Grant-in-Aid for Scientific Research from the Ministry of Education, Culture, Sports, Science, and Technology, Japan.

References

[1] T. Urade, T. Iemori, M. Osawa, N. Nakayama, and I. Morita, "Protecting layer for the dielectric in ac plasma panels," *IEEE Transactions on Electron Devices*, vol. 23, no. 3, pp. 313–318, 1976.

[2] S. Valeri, S. Altieri, A. Di Bona, C. Giovanardi, and T. S. Moia, "Structural study of thin MgO layers on Ag(001) prepared by either MBE or sputter deposition," *Thin Solid Films*, vol. 400, no. 1-2, pp. 16–21, 2001.

[3] S. A. Chambers, Y. Gao, and Y. Liang, "The early stages of MgO epitaxy on lattice-matched Cr0.7Mo0.3(001)," *Surface Science*, vol. 339, no. 3, pp. 297–309, 1995.

[4] P. Ghekiere, S. Mahieu, G. de Winter, R. de Gryse, and D. Depla, "Scanning electron microscopy study of the growth mechanism of biaxially aligned magnesium oxide layers grown by unbalanced magnetron sputtering," *Thin Solid Films*, vol. 493, no. 1-2, pp. 129–134, 2005.

[5] K. P. Kalyanikutty, F. L. Deepak, C. Edem, A. Govindaraj, and C. N. R. Rao, "Carbon-assisted synthesis of nanowires and related nanostructures of MgO," *Materials Research Bulletin*, vol. 40, no. 5, pp. 831–839, 2005.

[6] S. Stankic, M. Müller, O. Diwald, M. Sterrer, E. Knözinger, and J. Bernardi, "Size-dependent optical properties of MgO nanocubes," *Angewandte Chemie International Edition*, vol. 44, no. 31, pp. 4917–4920, 2005.

[7] Y. Zhang, Z. Huang, F. Tang, and J. Ren, "Ferrite hollow spheres with tunable magnetic properties," *Thin Solid Films*, vol. 515, no. 4, pp. 2555–2561, 2006.

[8] Y. Tan, C. Li, Y. Wang, J. Tang, and X. Ouyang, "Fast-response and high sensitivity gas sensors based on SnO_2 hollow spheres," *Thin Solid Films*, vol. 516, no. 21, pp. 7840–7843, 2008.

[9] C. Chang, M. Tsai, G. Chen, M. Wu, and T. Hung, "Preparation and properties of porous polyimide films with

TiO_2/polymer double shell hollow spheres," *Thin Solid Films*, vol. 517, no. 17, pp. 4966–4969, 2009.

[10] J. Moon, J. Park, S. Lee, and T. Zyung, "Colloidal templating for producing hollow ZnO shells: fabrication, growth and electrical properties," *Thin Solid Films*, vol. 517, no. 14, pp. 3904–3907, 2009.

[11] K.-Y. Niu, J. Yang, J. Sun, and X.-W. Du, "One-step synthesis of MgO hollow nanospheres with blue emission," *Nanotechnology*, vol. 21, no. 29, article 295604, 2010.

[12] T. Muraoka and S. Iizuka, "MgO microparticle deposition by radio frequency impulse discharge in a small-diameter tube," *Japanese Journal of Applied Physics*, vol. 48, no. 2, Article ID 025501, 4 pages, 2009.

[13] T. Muraoka, T. Kashimura, and S. Iizuka, "Spherical MgO microparticle deposition by RF impulse discharge with small coaxial electrodes," *Thin Solid Films*, vol. 518, no. 3, pp. 1012–1015, 2009.